

SupScene: Learning Overlap-Aware Global Descriptor for Unconstrained SfM

Xulei Shi¹, Maoyu Wang¹, Yuning Peng¹, Guanbo Wang¹, Xin Wang¹, Qi Chen², Pengjie Tao¹

Abstract— Image retrieval is a critical step for alleviating the quadratic complexity of image matching in unconstrained Structure-from-Motion (SfM). However, in this context, image retrieval typically focuses more on the image pairs of geometric matchability than on those of semantic similarity, a nuance that most existing deep learning-based methods guided by batched binaries (overlapping vs. non-overlapping pairs) fail to capture. In this paper, we introduce *SupScene*, a novel solution that learns global descriptors tailored for finding overlapping image pairs of similar geometric nature for SfM. First, to better underline co-visible regions, we employ a subgraph-based training strategy that moves beyond equally important isolated pairs, leveraging ground-truth geometric overlapping relationships with various weights to provide fine-grained supervision via a soft supervised contrastive loss. Second, we introduce DiVLAD, a DINO-inspired VLAD aggregator that leverages the inherent multi-head attention maps from the last block of ViT. And then, a learnable gating mechanism is designed to adaptively utilize these semantically salient cues with visual features, enabling a more discriminative global descriptor. Extensive experiments on the GL3D dataset demonstrate that our method achieves state-of-the-art performance, significantly outperforming NetVLAD while introducing a negligible number of additional trainable parameters. Furthermore, we show that the proposed training strategy brings consistent gains across different aggregation techniques. Code and models are available at <https://anonymous.4open.science/r/SupScene-5B73>.

I. INTRODUCTION

SfM is a fundamental technique in 3D reconstruction, enabling the generation of accurate 3D models from both ordered and unordered image sets. However, its application to ever-growing image collections is hampered by the image matching bottleneck, which has a quadratic time complexity [1]. To mitigate this, overlapping image retrieval is crucial for pre-selecting candidate pairs, drastically reducing the search effort for local feature matching which is subsequently employed for geometrical processing.

In recent years, ample works have been studied on learning compact global features for image retrieval or identifying overlapping image pairs. Some early endeavors have been spent on investigating CNN-based global features, such as VGG [2] and ResNet [3] with various aggregation strategies for global descriptors [4], [5], [6], [7], [8]. With the emergence of Vision Transformers (ViTs) [9], Transformer-based global descriptor gains more interest in the field [10], [11]. Among these, DINOv2 [12] is proved to extract robust and generalized visual feature through self-supervision, serving as a very promising feature extractor in more recent studies [13], [14].

Despite these extensive works, learning global descriptor for the task of SfM presents distinctive challenges that

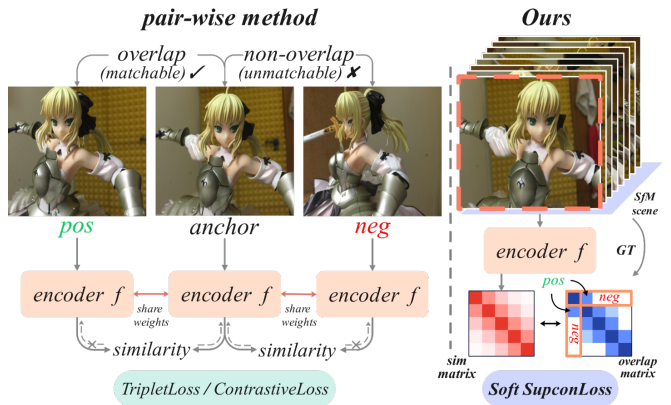


Fig. 1: Pair-wise methods vs. SupScene. Left: conventional pair-wise metric learning relies on isolated triplets (anchor, positive, negative) and optimizes with pairwise losses (e.g., Triplet Loss), capturing only one-to-one relationships. In contrast, our SupScene constructs training batches from overlapping subgraphs of co-visible image pairs in SfM. A weight-shared encoder processes the entire subgraph to produce a dense feature similarity matrix, which is directly supervised by the ground-truth geometric overlap matrix via a soft supervised contrastive loss.

distinguish it from general image retrieval. SfM employs image pairs of geometric matchability, not just those of semantic similarity. While images within a specific scene are often semantically related, this is not a sufficient condition for a valid matchable pair. For instance, the different areas of a scene may appear semantically similar but geometrically unmatchable, which means the global descriptor should be more sensitive to geometric overlap rather than semantic content.

While advanced backbones such as DINOv2 are capable of extracting rich visual representations, conventional pair-wise training strategies (e.g., MIRorR[15], SiaMAC[16] and LOIP[17]) still impose limitations. As illustrated in Fig. 1, these approaches rely on isolated image pairs (anchor, positive, negative) for metric learning, thereby providing only coarse, binary supervision (i.e., overlap vs. non-overlap) while neglecting the diverse many-to-many geometric overlapping relationships that are intrinsic to SfM. Moreover, a second challenge arises from how these powerful backbones are utilized. Beyond patch-level features, ViT-based models provide multi-head self-attention maps that capture high-level semantic context. Effectively integrating such information can significantly enhance the discriminative power of

the resulting global descriptor.

To overcome these limitations, we propose SupScene, a novel framework for learning global descriptors that is specifically designed to leverage the inherent overlapping relationships required by SfM. Our main contributions are threefold:

- A new training strategy that shifts from image pairs to cohesive scene subgraphs is proposed. These subgraphs, derived from SfM data, are optimized with an overlap-aware contrastive loss(Soft SupConLoss) that leverages ground-truth overlap scores to provide fine-grained geometric supervision.
- We design DiVLAD (DINO-inspired VLAD), a novel aggregator that synergistically utilizes both the visual features and the implicit semantic context encoded in the attention maps of the DINOv2 backbone.
- Specifically within DiVLAD, we introduce a learnable, cluster-adaptive gating mechanism. This allows each cluster to learn an adaptive strategy for dynamically selecting and fusing the most salient attention head weights, significantly enhancing the descriptor’s discriminative power.

II. RELATED WORKS

A. Image Retrieval for Structure-from-Motion

Global descriptor evolution. Early work in SfM-oriented image retrieval primarily relied on handcrafted local features [18], [19], [20], which were aggregated into global descriptors using encoding methods such as Bag-of-Words [21], [22], [23] and its more sophisticated variants, including Vector of Locally Aggregated Descriptors(VLAD) [24], [25], [26] and Fisher Vectors [27]. These vocabulary tree-based methods [28], [29] became a standard component in SfM pipelines and remain integral to systems like COLMAP [30]. While effective, the demand for greater robustness to extreme viewpoint and appearance changes prompted a shift towards learned representations. This began with fine-tuning pre-trained CNNs with retrieval-specific objectives, which was shown to significantly boost performance [16], [6]. This progress led to modern hierarchical frameworks like HLoc [31], where a learned global descriptor first retrieves candidate pairs, and is followed by precise local feature matching and geometric verification.

Geometric supervision and training strategy. To achieve this, a key strategy involves leveraging geometric overlap signals from 3D reconstructions as direct supervision. Radenović et al. [32] and Shen et al. [15] reconstructed 3D scenes to reproject overlap information, using it as supervision to train retrieval models. Both methods adopt a pair-wise training strategy: the former used a Siamese network with contrastive loss, while the latter adopted a triplet loss along with a regional coding module. Although effective, such pair-wise approaches typically rely on simple binary positive/negative pairs, such coarse supervision fails to capture the nuanced degrees of geometric overlap between images. Another line of work incorporates structural information

more explicitly. For example, methods like IMvGCN [33] use Graph Convolutional Networks (GCNs) to refine matching graphs by introducing topological constraints derived from overlap cues.

B. Global Feature Aggregation for Image Retrieval

While early methods used features from fully-connected layers, it was quickly established that features from convolutional layers offer a better balance of semantic abstraction and spatial preservation [34], [35]. The focus of modern retrieval research has largely centered on how to effectively aggregate deep spatial feature maps into a compact and discriminative global vector [36]. Methods like R-MAC [4], SPoC [37], and CroW [38] learn to weight and pool features from salient image regions [39]. By generalizing both average and max pooling, Generalized Mean (GeM) pooling [6] has become a foundational component in many state-of-the-art retrieval pipelines [40], [41], [42], [36].

Another major paradigm is based on learnable clustering. NetVLAD [5] replaced VLAD’s hard assignment with a differentiable soft-assignment version, enabling end-to-end training and inspiring many variants [43], [7], [17]. Further extending this idea, SALAD [44] employs an optimal transport formulation solved via the Sinkhorn algorithm with dustbin to focus on semantically discriminative regions. Recently, methods like AnyLoc [45] combined frozen DINOv2 features with VLAD aggregation, demonstrating strong zero-shot retrieval ability. Notably, the exceptional performance of DINOv2 [13], [14] has firmly validated the power of its visual representation ability for retrieval task. This success has naturally shifted the research focus from simply using the final output features to a more nuanced question: how to fully and efficiently harness the rich, structured representations available within the Transformer’s internal layers.

Concurrently, feedforward and end-to-end SfM pipelines such as VGGT[46] and Light3R-SFM[47] have shown promise in efficiently reconstructing scenes from unconstrained images. While promising, they remain constrained by reconstruction accuracy and computational overhead. Inspired by this feedforward paradigm, we extend the idea into a novel training framework that uses dense overlapping subgraphs for fine-grained and efficient supervision.

III. METHODOLOGY

Given a collection of images from a SfM dataset, where sequences are typically captured around a cohesive 3D structure or scene with substantial overlap between consecutive views. This intrinsic property dictates that a discriminative global descriptor must be highly sensitive to the salient, repeatable features that constitute these key overlapping regions.

In section A, as illustrated in Fig. 1, the SupScene framework moves beyond discrete pairs, instead processing entire subgraphs of co-visible images at once. By treating the dense co-visibility graph as a fine-grained supervisory signal, it compels the network to learn, in an end-to-end fashion, the visual cues indicative of geometric overlap. This

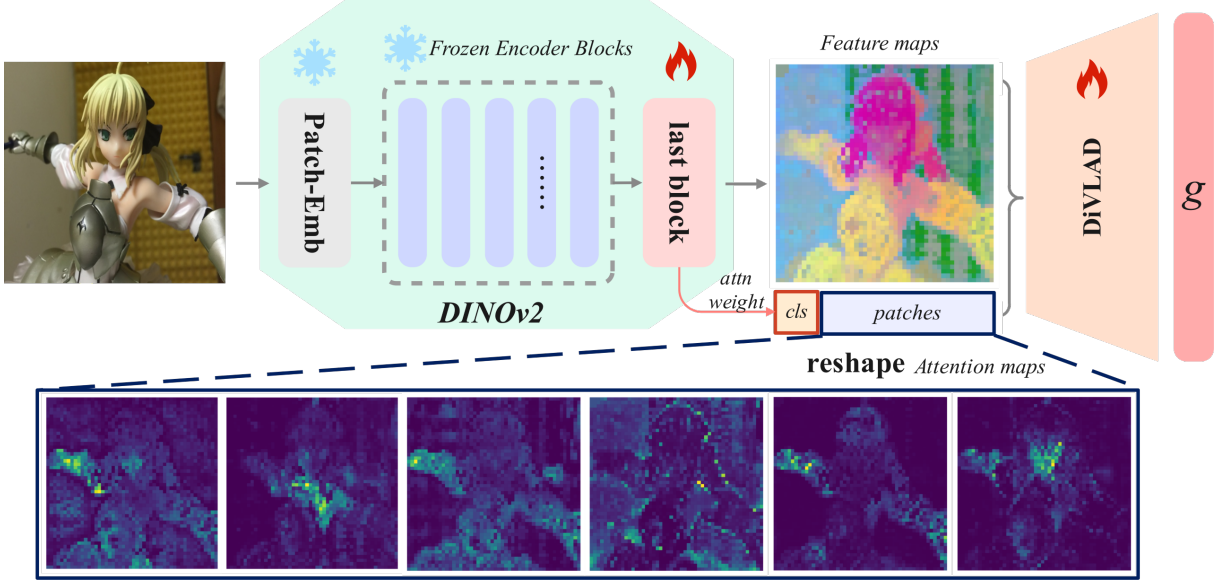


Fig. 2: The overall architecture for extracting our global descriptor. An input image is tokenized into patch tokens by DINOv2; all encoder blocks are frozen except the last (trainable), whose $cls \rightarrow$ patch attention provides per-patch importance. Patch tokens are reshaped into a feature map and aggregated by the proposed DiVLAD, which utilizes multi-head attention maps from DINOv2 to adaptively reweight token contributions during VLAD aggregation, ultimately producing a discriminative compact global descriptor g .

enables the model to learn from abundant many-to-many geometric constraints within local scenes, yielding more robust global descriptors for SfM image retrieval. In section B, the proposed DiVLAD module harnesses the multi-level semantic context of multi-head attention (MHA). By effectively identifying, weighting, and aggregating these features, DiVLAD constructs a global descriptor that is inherently attuned to the scene’s underlying overlapping relationship.

A. *SupScene: Overlap-Aware Supervised Training Framework*

Data organization and subgraph sampling. We model each 3D scene as overlap graph $\mathcal{G} = (\mathcal{V}, \mathcal{E}, w)$, where the vertex set $\mathcal{V} = \{v_1, \dots, v_{N_S}\}$ represents the N_S images of the scene. An edge $(v_i, v_j) \in \mathcal{E}$ indicates significant geometric overlap between images i and j , with weight $w_{ij} \in [0, 1]$ quantifying the overlap ratio derived from the 3D reconstruction.

For each training batch, we sample a subgraph $\mathcal{G}_{\mathcal{B}} \subset \mathcal{G}$ with n nodes, $\mathcal{V}_{\mathcal{B}} = v_{i_1}, \dots, v_{i_n}$. The ground-truth supervision signal is the induced overlap matrix $\mathbf{O} \in [0, 1]^{n \times n}$, defined as:

$$\mathbf{O}_{jk} = \begin{cases} w_{i_j i_k} & \text{if } (v_{i_j}, v_{i_k}) \in \mathcal{E}, \\ 1 & \text{if } j = k, \\ 0 & \text{otherwise.} \end{cases} \quad (1)$$

The sampling strategy aims to construct batches with meaningful geometric relationships. We employ two strategies:

- **Anchor Expansion:** Begins with a random anchor node and performs breadth-first search(BFS) along high-confidence edges with $w_{ij} \geq \tau_{iou}$, forming a connected

subgraph of spatially proximate, highly overlapping images, providing meaningful positive examples.

- **Balanced Sampling:** Iteratively optimizes a randomly initialized node set via greedy swaps to achieve a target positive-pair ratio ρ . This guarantees a sufficient number of non-trivial positive pairs in each batch, mitigating issues arising from sparse connectivity.

In instances where a scene contains fewer than n images ($N_S < n$), the batch is padded to size n with null data, and a corresponding mask is generated to exclude padded elements from the loss calculation. For each scene, we sample $T_i = N_S | n + 1$ times with distinct anchors and take $\sum T_i$ as the total batch count.

Forward and overlap-aware optimization. The sampled image subgraph $\mathcal{V}_{\mathcal{B}}$ is processed through a shared-weight encoder $f(\cdot)$ (e.g., DINOv2 with an aggregation module), producing a set of feature tensors. For our DiVLAD, As depicted in Fig. 2, given an input image, the backbone produces two key outputs from its last block: (1)A feature map $\mathbf{F} \in \mathbb{R}^{C \times H \times W}$ of patch embeddings. (2)A MHA map $\mathbf{A}_{attn} \in \mathbb{R}^{N_h \times H \times W}$, computed from the attention weights between the cls token and all patch tokens. The attention for a single head is given by:

$$\mathbf{A}_{attn}^{(h)} = \text{softmax} \left(\frac{\mathbf{q}_{cls}^{(h)} (\mathbf{K}_{patches}^{(h)})^T}{\sqrt{d_k}} \right) \quad (2)$$

where $\mathbf{q}_{cls}^{(h)}$ and $\mathbf{K}_{patches}^{(h)}$ are the query (from the cls token) and key (from the patches) vectors for head h , respectively.

These outputs are fused by the DiVLAD module to produce a compact global descriptor g for each image. For a subgraph of n images, we obtain a set of global descriptors

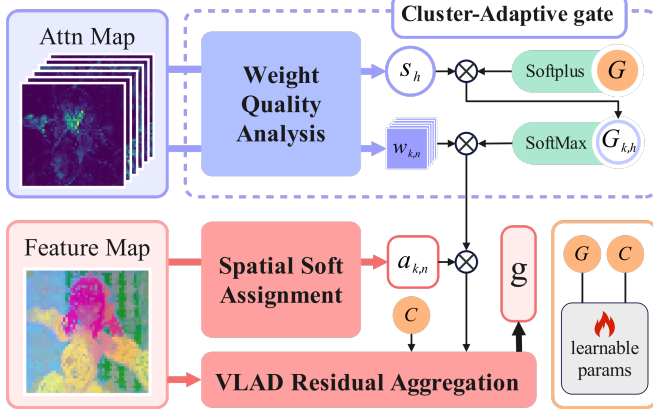


Fig. 3: Detailed architecture of the DiVLAD aggregator. The module extends NetVLAD by introducing a cluster-adaptive gate. This gate analyzes multi-head attention maps to generate a semantic modulation weight, which is fused with the standard spatial soft assignment ($a_{k,n}$). This process guides the final VLAD residual aggregation, ensuring it prioritizes features from semantically salient regions.

$\mathbf{g}_1, \dots, \mathbf{g}_n$. Their pairwise cosine similarities form a matrix $\mathbf{S} \in \mathbb{R}^{n \times n}$. The model is optimized by minimizing a Soft SupConLoss \mathcal{L} , which aligns \mathbf{S} with the GT overlap matrix \mathbf{O} , ensuring semantic similarity reflects geometric overlap.

Inference. The proposed method is computationally efficient for inference. A single image is processed independently through the network during inference to generate its descriptor, ensuring efficient large-scale retrieval.

B. DINO-inspired VLAD (DiVLAD)

The proposed DiVLAD aggregator synergistically utilizes the rich visual tokens \mathbf{x}_n and the multi-head attention maps $A_{h,n}$ from the DINOv2 backbone. As illustrated in Fig. 3, it extends the standard NetVLAD architecture by incorporating a novel gating mechanism.

Spatial assignment. Following the standard NetVLAD framework, a lightweight convolutional head first processes the input \mathbf{x}_n to produce a soft assignment map $a_{k,n}$, indicating the initial affinity of each pixel to our K clusters based on visual appearance.

Cluster-adaptive gating. The core of DiVLAD is a learnable gating mechanism that modulates and harnesses the multi-head DINOv2 attention maps. For each attention head h , we compute a token-wise quality score:

$$w_{h,n} = \sigma \left(\frac{A_{h,n} - \mu_h}{\sigma_h} \right)^{\gamma_g} \quad (3)$$

where $\sigma(\cdot)$ is the sigmoid function and γ_g controls the sharpness, which is set to 0.5 empirically. Additionally, we compute an image-level head confidence score s_h that combines the average quality and low entropy of each head's attention distribution. These scores are combined via a learned gating matrix $\mathbf{G} \in \mathbb{R}^{K \times H_h}$ to produce cluster-

specific weights:

$$s_h = \frac{1}{N} \sum_{n=1}^N w_{h,n} \cdot (1 - \text{entropy}_h) \quad (4)$$

$$g_{k,h} \propto \text{softplus}(\mathbf{G}_{k,h}) \cdot s_h \quad (5)$$

Gated VLAD aggregation. The final aggregation fuses both spatial assignment and semantic modulation:

$$\mathbf{v}_k = \sum_n a_{k,n} \cdot \left(\sum_h g_{k,h} \cdot w_{h,n} \right) \cdot (\mathbf{x}_n - \mathbf{c}_k) \quad (6)$$

The resulting VLAD vectors subsequently form the final global descriptor \mathbf{g} . By directly incorporating the attention maps into the aggregation process, our method enables gradients to flow directly back to fine-tune the backbone's final block. This promotes the learning of more semantically meaningful and geometrically aligned attention patterns, which in turn further enhances the quality of the aggregated descriptors. This dual-promotion mechanism creates a virtuous co-adaptation cycle between feature extraction and feature aggregation, leading to synergy improvement in both components.

C. Soft SupConLoss

We adopt a soft supervised contrastive learning objective to align the semantic similarity between image descriptors with their geometric overlap.

Formally, for a batch of n images with pairwise overlap matrix $\mathbf{O} \in [0, 1]^{n \times n}$ and predicted similarity matrix $\mathbf{S} \in [-1, 1]^{n \times n}$, a soft weight matrix $\mathbf{W} \in \mathbb{R}^{n \times n}$ is constructed as:

$$\mathbf{W}_{ij} = \begin{cases} \mathbf{O}_{ij}^{\gamma_s} & \text{if } \mathbf{O}_{ij} \geq \tau_{iou} \\ \mathbf{O}_{ij}^{1/\gamma_s} & \text{if } 0 < \mathbf{O}_{ij} < \tau_{iou} \\ 0 & \text{otherwise} \end{cases} \quad (7)$$

where τ_{iou} is the positive threshold and γ_s is a focusing parameter, we set $\gamma_s = 0.7$ empirically to amplify the distinction between hard positive and negative samples. The final soft supervised contrastive loss is computed as:

$$\mathcal{L} = \frac{1}{|\mathcal{V}|} \sum_{i \in \mathcal{V}} \left(-\frac{1}{Z_i} \sum_j \mathbf{W}_{ij} \log \frac{\exp(\mathbf{S}_{ij}/t)}{\sum_{k \neq i} \exp(\mathbf{S}_{ik}/t)} \right) \quad (8)$$

where \mathcal{V} represents the set of valid anchor and $Z_i = \sum_j \mathbf{W}_{ij}$ is the normalization factor for anchor i , t is a temperature parameter.

IV. EXPERIMENT

In this section, we conduct a thorough evaluation to validate the effectiveness of our proposed SupScene training framework and the DiVLAD aggregation module. We first detail the implementation setup and evaluation metrics. This is followed by a comparative analysis against existing state-of-the-art methods to assess the performance of our approach. Finally, we perform ablation studies and present qualitative results to provide further insight into the model's behavior.

A. Implementation Details

We provide the implementation specifics for reproducing our experiments. The proposed framework, as detailed in Sec. 3, is implemented using PyTorch.

Dataset and training configuration. The model is trained on the GL3D dataset[48], a large-scale dataset originally designed for multi-view stereo and SfM tasks. In line with common practices in image retrieval for SfM, we adapt this dataset for the image retrieval task by leveraging its scene metadata to define positive image pairs. Specifically, following the protocol outlined in IMvGCN[33], we consider image pairs with a mesh-reprojection overlap τ_{iou} exceed 0.25 as effective matches. Our training set comprises 110k images from 503 scenes, excluding all images from the official test set of 40 scenes (8,914 images), which is used exclusively for evaluation.

TABLE I: Comparison against retrieval techniques on GL3D dataset. The first three baselines are re-implemented following the experimental setup in MIRorR. For IMvGCN, only recall metrics are reported as no implementation is available. Both our method and baseline(avgpool) are trained within our unified framework for fair comparison.

Method	Backbone	Dim	Recall		mAP	
			@25	@100	@25	@100
SiaMAC[32]	CNN-Based	512	59.4	88.6	63.3	66.2
NetVLAD[5]	CNN-Based	16384	58.8	87.8	61.7	64.1
MIRorR[15]	CNN-Based	256	61.1	90.3	69.1	73.4
IMvGCN[33]	CNN-Based	2048	70.8	70.8	—	—
AVG	DINOv2	768	71.5	96.6	77.7	80.3
DiVLAD	DINOv2	24576	73.0	97.2	79.8	82.2

We employ a soft variant of the SupConLoss, which offers improved generalization compared to the standard SupConLoss loss. The model is optimized using AdamW with an initial learning rate of 0.0002. A linear warm-up is applied for the first 10% of the training steps, followed by cosine annealing for learning rate decay. Training is conducted over 50 epochs with image resizing to 322×322 pixels.

All experiments are conducted in a distributed data-parallel setting across 8 NVIDIA RTX A6000 GPUs. Due to the high memory demands of subgraph sampling with a size of 128, the maximum batch size per GPU is set to 2.

Architecture and attention configuration. We employ DINOv2-B as our image encoder, selected for its strong performance and computational efficiency suitable for SfM-based retrieval tasks. All blocks except the last are frozen to balance efficiency and representation learning. For our DiVLAD aggregation, we leverage the attention mechanism from this trainable final block. Specifically, we extract the attention weights from the *cls* token to all patch tokens and reshape them into a spatial map of dimension (B, nH, H, W) , which directly guides the feature aggregation process.

Evaluation metrics. We adopt Recall@k, mean Average Precision(mAP)@k, and Normalized Discounted Cumulative Gain(NDCG)@k as our evaluation metrics, with a particular emphasis on retrieval-oriented formulations. Unlike some variants used in visual localization, our Recall@k calculation follows the standard information retrieval convention: the denominator includes all relevant images in the database, thereby measuring the ability to retrieve every possible positive match. This offers a comprehensive assessment of recall performance, especially in scenarios where multiple overlapping reference images exist per query. To ensure consistency with the evaluation protocol of MIRorR, all retrieval results are obtained using full-scale retrieval over the entire test set.

B. Comparison with previous works on GL3D

We comprehensively compare our method against several representative baselines for image retrieval on the GL3D dataset, including SiaMAC[32], NetVLAD, MIRorR[15], and IMvGCN. As our approach performs single-stage retrieval, we restrict the comparison to global feature retrieval methods. Results of comparison methods are obtained using their officially recommended configurations.

The results are detailed in Table I, the strong visual representations provided by the DINOv2 backbone enable even our baseline model with average pooling to surpass all previous methods across all metrics. Building upon this foundation, the proposed DiVLAD aggregation mechanism further enhances retrieval performance, achieving new state-of-the-art results on the GL3D dataset.

C. Comparison with advanced aggregation methods

We compare the proposed DiVLAD aggregation module against several state-of-the-art global feature aggregation methods, including GeM [6], NetVLAD [5], and DINOv2 SALAD [44]. To ensure a fair comparison, all these methods are built upon the same DINOv2 backbone and trained within our SupScene framework.

The results in Table II first highlight the effectiveness of our training strategy, as all methods show significant performance gains when trained within our framework. On top of this strong baseline, our proposed DiVLAD delivers competitive performance, achieving the highest scores in Recall@50, Recall@100, mAP@100, and NDCG@50/100. Notably, it delivers comparable results to the state-of-the-art single-stage retrieval method, DINOv2 SALAD, in terms of Recall@25 and mAP@25.

D. Result of SfM Reconstruction.

Beyond retrieval metrics, we evaluated our method’s direct impact on a downstream SfM task using three public internet photo collections [49]. We employed the candidate image pairs generated from the top-100 retrieval results of each method as input to the SfM pipeline and evaluated the number of successfully registered images. As shown in Table III, our method leads to the highest number of registered images across all datasets. This indicates that our retrieval

TABLE II: **Comparison of state-of-the-art aggregation methods.** All methods are built upon a DINOv2 backbone. The first two rows show results from officially released models, and remaining methods are trained within our framework. For DINOv2 SALAD, we fine-tuning the official weights within our framework.

Method	Desc. size	Recall			mAP			NDCG		
		@25	@50	@100	@25	@50	@100	@25	@50	@100
DINOv2 AVG	768	61.6	75.6	87.3	64.1	63.5	66.0	76.9	78.6	83.3
DINOv2 SALAD	8448	64.8	76.5	86.2	68.9	67.4	69.2	80.1	80.5	84.2
DINOv2 AVG	768	71.5	87.0	96.6	77.7	78.0	80.3	86.6	88.7	92.2
DINOv2 GeM	768	71.9	87.1	96.6	78.2	78.1	80.1	87.1	88.7	92.2
DINOv2 NetVLAD	24576	72.5	87.7	97.0	79.0	79.3	81.5	87.5	89.4	92.8
DINOv2 SALAD	8448	73.0	87.7	96.5	79.7	79.6	81.6	88.0	89.6	92.8
DINOv2 DiVLAD(ours)	24576	73.0	88.2	97.2	79.8	80.0	82.2	88.0	89.9	93.2

TABLE III: SfM results on several 1DSfM dataset.

Scene	Method	Image numbers	Registered images \uparrow	Mean track length \uparrow	Mean reproj. error (px) \downarrow
Gendarmenmarkt	SiaMAC	1463	977	6.48	0.722
	MIRorR		980	6.46	0.721
	IMvGCN		997	6.27	0.693
	Ours		1048	6.47	0.715
Madrid Metropolis	SiaMAC	1344	428	7.28	0.619
	MIRorR		489	7.22	0.590
	IMvGCN		420	7.16	0.610
	Ours		491	7.32	0.618
Alamo	SiaMAC	2915	904	11.95	0.661
	MIRorR		925	12.20	0.636
	IMvGCN		862	12.02	0.632
	Ours		972	12.39	0.642

TABLE IV: **Ablation study on the loss function and gate.**

Method	Recall@25	mAP@25
DINOv2 AVG (SupConLoss)	70.9	77.1
DINOv2 DiVLAD (SupConLoss)	72.3	78.9
DINOv2 DiVLAD w/o Gate	72.7	79.6
DINOv2 AVG	71.5	77.7
DINOv2 DiVLAD (ours)	73.0	79.8

results contain a greater proportion of effective matches, which is essential for obtaining more complete and robust 3D reconstructions.

E. Ablation Studies

Effect of training strategy and configuration. We first compare the performance of our subgraph-level training framework SupScene with pair-wise method. As shown in Fig. 4 left, SupScene converges faster and reaches higher Recall@25; even with hard-negative mining, the pair-wise scheme remains below our configuration with $n_{sub} = 8$. We further ablate subgraph size n_{sub} and batch size B (Fig. 4 right). We observe that performance gains diminish when the subgraph size exceeds 32. This aligns with the distribution of positive samples in our dataset, where each image typically has 10–20 overlaps. In contrast, the impact of batch size is less pronounced. While larger batches yield minor gains in

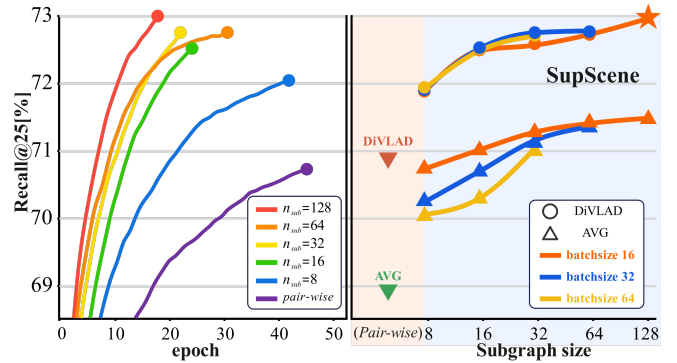


Fig. 4: **Analysis of training strategy and key hyperparameters.** We compare our subgraph-based SupScene framework against the pair-wise.(1)Left: shows the convergence behavior of Recall@25 for DiVLAD aggregator, and(2) details the final accuracy as a function of subgraph and batch size. The star marks the best observed setting.

DiVLAD, likely due to the stabilizing effect of BatchNorm within it. We adjusted the learning rate of $[5e-5, 1e-4]$ depending on different batch sizes, the subgraph size remains the dominant factor. This analysis suggests that prioritizing a larger subgraph size with a moderate batch size (e.g., 16) offers an optimal balance between performance and computational efficiency.

Compared with standard SupConLoss. We isolate the effect of overlap-aware weighting by replacing our soft loss with the standard SupConLoss, which treats all positive pairs equally(i.e., setting $W_{ij} = 1[O_{ij} > \tau_{iou}]$). Results in Table IV show that our soft weighting strategy consistently outperforms the standard loss. This confirms that weighting pairs based on their geometric overlap provides a more nuanced supervisory signal, leading to better similarity calibration and more robust descriptors.

Effect of learnable gate parameters. As shown in Table IV, even without the learnable gate (row 3), the incorporation of attention weights already yields clear improvements over the strong NetVLAD baseline in terms of both Recall and mAP, demonstrating the inherent value of the attention signals. Subsequently, the introduction of our learnable gate provides an additional performance boost. This incremental gain demonstrates the value of dynamically adapting the importance of each attention head per cluster, which allows the model to yield a more discriminative representation.

F. Visualization of the assignment map

To generate the visualizations, the assignment scores for all clusters at each spatial location are aggregated into a single-channel map. This map is then resized to the original image dimensions and overlaid as a heatmap.

A qualitative comparison of the heatmaps in Fig. 5 reveals the distinct behavior of each method. NetVLAD tends to activate on broad, texturally rich areas, which can sometimes be non-distinctive (e.g., the foliage in the first row). SALAD is often more sparse and focused, highlighting a few salient points, but can miss broader contextual regions. In contrast, our DiVLAD learns to identify regions most critical for the SfM retrieval task. As seen across all examples, its activations are not just semantically coherent—concentrating on the central temple or unique architecture but are focused on structures that offer high potential for geometric overlap and are semantically stable across viewpoint changes. This enhancement arises from leveraging the semantic information implicit in the attention weights, which guides the aggregator to prioritize regions that offer the most robust cues for establishing geometric correspondence across multiple views.

V. CONCLUSIONS

In this work, we introduce SupScene, a novel framework for learning global descriptors for unconstrained SfM. In particular, in contrast to other learning-based methods that take isolated image pairs as input training samples, a subgraph-based training solution that can fully leverage geometric overlap relationship is presented to improve the performance on finding overlapping image pairs. Then, a novel Dino-inspired VLAD(DiVLAD) aggregator is proposed, which incorporates implicit semantic cues from DINoV2 attention maps through a learned gating mechanism to emphasize features stable across multiple views. Extensive experiments on the GL3D benchmark demonstrate that our method achieves state-of-the-art performance in the tasks of both image retrieval and SfM. This innovative use of

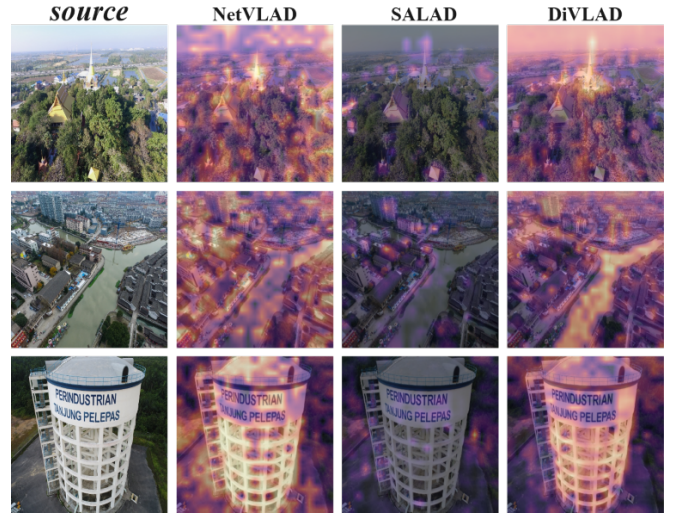


Fig. 5: **Assignment-map visualization.** Brighter regions indicate higher assignment scores, representing areas that contribute more significantly to the final global descriptor.

the DINoV2’s attention map provides a significant boost in retrieval performance. The success of this fusion principle confirms its potential, making its exploration within more advanced aggregation architectures a promising avenue for future research.

REFERENCES

- [1] X. Wang, F. Rottensteiner, and C. Heipke, “Structure from motion for ordered and unordered image sets based on random kd forests and global pose estimation,” *ISPRS Journal of Photogrammetry and Remote Sensing*, vol. 147, pp. 19–41, 2019.
- [2] K. Simonyan and A. Zisserman, “Very deep convolutional networks for large-scale image recognition,” *arXiv preprint arXiv:1409.1556*, 2014.
- [3] K. He, X. Zhang, S. Ren, and J. Sun, “Deep residual learning for image recognition,” in *Proceedings of the IEEE Conference on Computer Vision and Pattern Recognition (CVPR)*, June 2016.
- [4] G. Tolias, R. Sicre, and H. Jégou, “Particular object retrieval with integral max-pooling of cnn activations,” in *ICLR 2016-International Conference on Learning Representations*, 2016, pp. 1–12.
- [5] R. Arandjelovic, P. Gronat, A. Torii, T. Pajdla, and J. Sivic, “Netvlad: Cnn architecture for weakly supervised place recognition,” in *Proceedings of the IEEE Conference on Computer Vision and Pattern Recognition (CVPR)*, June 2016.
- [6] F. Radenović, G. Tolias, and O. Chum, “Fine-tuning cnn image retrieval with no human annotation,” *IEEE transactions on pattern analysis and machine intelligence*, vol. 41, no. 7, pp. 1655–1668, 2018.
- [7] S. Hausler, S. Garg, M. Xu, M. Milford, and T. Fischer, “Patch-netvlad: Multi-scale fusion of locally-global descriptors for place recognition,” in *Proceedings of the IEEE/CVF Conference on Computer Vision and Pattern Recognition (CVPR)*, June 2021, pp. 14141–14152.
- [8] A. Ali-bey, B. Chaib-draa, and P. Giguère, “Mixvpr: Feature mixing for visual place recognition,” in *Proceedings of the IEEE/CVF Winter Conference on Applications of Computer Vision (WACV)*, January 2023, pp. 2998–3007.
- [9] A. Dosovitskiy, L. Beyer, A. Kolesnikov, D. Weissenborn, X. Zhai, T. Unterthiner, M. Dehghani, M. Minderer, G. Heigold, S. Gelly *et al.*, “An image is worth 16x16 words: Transformers for image recognition at scale,” in *International Conference on Learning Representations*, 2020.
- [10] P. Weinzaepfel, T. Lucas, D. Larlus, and Y. Kalantidis, “Learning super-features for image retrieval,” *arXiv preprint arXiv:2201.13182*, 2022.

[11] W. Song, R. Yan, B. Lei, and T. Okatani, "Globalizing local features: Image retrieval using shared local features with pose estimation for faster visual localization," in *2024 IEEE International Conference on Robotics and Automation (ICRA)*. IEEE, 2024, pp. 6290–6297.

[12] M. Oquab, T. Darcret, T. Moutakanni, H. Vo, M. Szafraniec, V. Khalidov, P. Fernandez, D. Haziza, F. Massa, A. El-Nouby *et al.*, "Dinov2: Learning robust visual features without supervision," *arXiv preprint arXiv:2304.07193*, 2023.

[13] G. Kordopatis-Zilos, V. Stojnić, A. Manko, P. Suma, N.-A. Ypsilantis, N. Efthymiadis, Z. Laskar, J. Matas, O. Chum, and G. Tolias, "Ilias: Instance-level image retrieval at scale," in *Proceedings of the Computer Vision and Pattern Recognition Conference (CVPR)*, June 2025, pp. 14 777–14 787.

[14] Y. Nozawa, Y.-C. Lin, K. Nakamura, and Y. Ng, "Prompt-guided attention head selection for focus-oriented image retrieval," in *Proceedings of the Computer Vision and Pattern Recognition Conference (CVPR) Workshops*, June 2025, pp. 4131–4141.

[15] T. Shen, Z. Luo, L. Zhou, R. Zhang, S. Zhu, T. Fang, and L. Quan, "Matchable image retrieval by learning from surface reconstruction," in *Asian conference on computer vision*. Springer, 2018, pp. 415–431.

[16] F. Radenović, G. Tolias, and O. Chum, "Cnn image retrieval learns from bow: Unsupervised fine-tuning with hard examples," in *European conference on computer vision*. Springer, 2016, pp. 3–20.

[17] Q. Hou, R. Xia, J. Zhang, Y. Feng, Z. Zhan, and X. Wang, "Learning visual overlapping image pairs for sfm via cnn fine-tuning with photogrammetric geometry information," *International Journal of Applied Earth Observation and Geoinformation*, vol. 116, p. 103162, 2023.

[18] D. G. Lowe, "Distinctive image features from scale-invariant keypoints," *International journal of computer vision*, vol. 60, no. 2, pp. 91–110, 2004.

[19] H. Bay, A. Ess, T. Tuytelaars, and L. Van Gool, "Speeded-up robust features (surf)," *Computer vision and image understanding*, vol. 110, no. 3, pp. 346–359, 2008.

[20] E. Rublee, V. Rabaud, K. Konolige, and G. Bradski, "Orb: An efficient alternative to sift or surf," in *2011 International conference on computer vision*. Ieee, 2011, pp. 2564–2571.

[21] G. Csurka, C. Dance, L. Fan, J. Willamowski, and C. Bray, "Visual categorization with bags of keypoints," in *Workshop on statistical learning in computer vision, ECCV*, vol. 1, no. 1-22. Prague, 2004, pp. 1–2.

[22] D. Nister and H. Stewenius, "Scalable recognition with a vocabulary tree," in *2006 IEEE Computer Society Conference on Computer Vision and Pattern Recognition (CVPR'06)*, vol. 2. Ieee, 2006, pp. 2161–2168.

[23] J. Philbin, O. Chum, M. Isard, J. Sivic, and A. Zisserman, "Object retrieval with large vocabularies and fast spatial matching," in *2007 IEEE conference on computer vision and pattern recognition*. IEEE, 2007, pp. 1–8.

[24] H. Jégou, M. Douze, C. Schmid, and P. Pérez, "Aggregating local descriptors into a compact image representation," in *2010 IEEE computer society conference on computer vision and pattern recognition*. IEEE, 2010, pp. 3304–3311.

[25] R. Arandjelovic and A. Zisserman, "All about vlad," in *Proceedings of the IEEE Conference on Computer Vision and Pattern Recognition (CVPR)*, June 2013.

[26] H. Jégou, F. Perronnin, M. Douze, J. Sánchez, P. Pérez, and C. Schmid, "Aggregating local image descriptors into compact codes," *IEEE transactions on pattern analysis and machine intelligence*, vol. 34, no. 9, pp. 1704–1716, 2011.

[27] F. Perronnin, Y. Liu, J. Sánchez, and H. Poirier, "Large-scale image retrieval with compressed fisher vectors," in *2010 IEEE Conference on Computer Vision and Pattern Recognition (CVPR)*. IEEE, 2010, pp. 3384–3391.

[28] J. Zheng, H. Fu, W. Li, W. Wu, L. Yu, S. Yuan, W. Y. W. Tao, T. K. Pang, and K. D. Kanniah, "Growing status observation for oil palm trees using unmanned aerial vehicle (uav) images," *ISPRS Journal of Photogrammetry and Remote Sensing*, vol. 173, pp. 95–121, 2021.

[29] S. Jiang, W. Jiang, and B. Guo, "Leveraging vocabulary tree for simultaneous match pair selection and guided feature matching of uav images," *ISPRS Journal of Photogrammetry and Remote Sensing*, vol. 187, pp. 273–293, 2022.

[30] J. L. Schonberger and J.-M. Frahm, "Structure-from-motion revisited," in *Proceedings of the IEEE Conference on Computer Vision and Pattern Recognition (CVPR)*, June 2016.

[31] P.-E. Sarlin, C. Cadena, R. Siegwart, and M. Dymczyk, "From coarse to fine: Robust hierarchical localization at large scale," in *Proceedings of the IEEE/CVF Conference on Computer Vision and Pattern Recognition (CVPR)*, June 2019.

[32] F. Radenović, G. Tolias, and O. Chum, "Cnn image retrieval learns from bow: Unsupervised fine-tuning with hard examples," in *European conference on computer vision*. Springer, 2016, pp. 3–20.

[33] S. Yan, M. Zhang, S. Lai, Y. Liu, and Y. Peng, "Image retrieval for structure-from-motion via graph convolutional network," *Information Sciences*, vol. 573, pp. 20–36, 2021.

[34] Y. Hou, H. Zhang, and S. Zhou, "Convolutional neural network-based image representation for visual loop closure detection," in *2015 IEEE international conference on information and automation*. IEEE, 2015, pp. 2238–2245.

[35] W. Chen, Y. Liu, W. Wang, E. M. Bakker, T. Georgiou, P. Fieguth, L. Liu, and M. S. Lew, "Deep learning for instance retrieval: A survey," *IEEE Transactions on Pattern Analysis and Machine Intelligence*, vol. 45, no. 6, pp. 7270–7292, 2022.

[36] S. Shao, K. Chen, A. Karpur, Q. Cui, A. Araujo, and B. Cao, "Global features are all you need for image retrieval and reranking," in *Proceedings of the IEEE/CVF International Conference on Computer Vision (ICCV)*, October 2023, pp. 11 036–11 046.

[37] A. Babenko and V. Lempitsky, "Aggregating local deep features for image retrieval," in *Proceedings of the IEEE International Conference on Computer Vision (ICCV)*, December 2015.

[38] Y. Kalantidis, C. Mellina, and S. Osindero, "Cross-dimensional weighting for aggregated deep convolutional features," in *European conference on computer vision*. Springer, 2016, pp. 685–701.

[39] A. S. Razavian, J. Sullivan, S. Carlsson, and A. Maki, "Visual instance retrieval with deep convolutional networks," *ITE Transactions on Media Technology and Applications*, vol. 4, no. 3, pp. 251–258, 2016.

[40] B. Cao, A. Araujo, and J. Sim, "Unifying deep local and global features for image search," in *European conference on computer vision*. Springer, 2020, pp. 726–743.

[41] M. Yang, D. He, M. Fan, B. Shi, X. Xue, F. Li, E. Ding, and J. Huang, "Dolg: Single-stage image retrieval with deep orthogonal fusion of local and global features," in *Proceedings of the IEEE/CVF International Conference on Computer Vision (ICCV)*, October 2021, pp. 11 772–11 781.

[42] S. Lee, H. Seong, S. Lee, and E. Kim, "Correlation verification for image retrieval," in *Proceedings of the IEEE/CVF Conference on Computer Vision and Pattern Recognition (CVPR)*, June 2022, pp. 5374–5384.

[43] R. Lin, J. Xiao, and J. Fan, "Nextvlad: An efficient neural network to aggregate frame-level features for large-scale video classification," in *Proceedings of the European Conference on Computer Vision (ECCV) Workshops*, September 2018.

[44] S. Izquierdo and J. Civera, "Optimal transport aggregation for visual place recognition," in *Proceedings of the IEEE/CVF Conference on Computer Vision and Pattern Recognition (CVPR)*, June 2024, pp. 17 658–17 668.

[45] N. Keetha, A. Mishra, J. Karhade, K. M. Jatavallabhula, S. Scherer, M. Krishna, and S. Garg, "Anyloc: Towards universal visual place recognition," *IEEE Robotics and Automation Letters*, vol. 9, no. 2, pp. 1286–1293, 2023.

[46] J. Wang, M. Chen, N. Karaev, A. Vedaldi, C. Rupprecht, and D. Novotny, "Vggt: Visual geometry grounded transformer," in *Proceedings of the Computer Vision and Pattern Recognition Conference (CVPR)*, June 2025, pp. 5294–5306.

[47] S. Elflein, Q. Zhou, and L. Leal-Taixé, "Light3r-sfm: Towards feed-forward structure-from-motion," in *Proceedings of the IEEE/CVF Conference on Computer Vision and Pattern Recognition (CVPR)*, June 2025, pp. 16 774–16 784.

[48] Y. Yao, Z. Luo, S. Li, J. Zhang, Y. Ren, L. Zhou, T. Fang, and L. Quan, "Blendedmvs: A large-scale dataset for generalized multi-view stereo networks," in *Proceedings of the IEEE/CVF Conference on Computer Vision and Pattern Recognition (CVPR)*, June 2020.

[49] K. Wilson and N. Snavely, "Robust global translations with 1dsfm," in *Proceedings of the European Conference on Computer Vision (ECCV)*, 2014.